

AERO: AUDIO SUPER RESOLUTION IN THE SPECTRAL DOMAIN

Moshe Mandel, Or Tal, Yossi Adi

School of Computer Science and Engineering
The Hebrew University of Jerusalem, Israel

ABSTRACT

We present AERO, a audio super-resolution model that processes speech and music signals in the spectral domain. AERO is based on an encoder-decoder architecture with U-Net like skip connections. We optimize the model using both time and frequency domain loss functions. Specifically, we consider a set of reconstruction losses together with perceptual ones in the form of adversarial and feature discriminator loss functions. To better handle phase information the proposed method operates over the complex-valued spectrogram using two separate channels. Unlike prior work which mainly considers low and high frequency concatenation for audio super-resolution, the proposed method directly predicts the full frequency range. We demonstrate high performance across a wide range of sample rates considering both speech and music. AERO outperforms the evaluated baselines considering Log-Spectral Distance, ViSQOL, and the subjective MUSHRA test. Audio samples and code are available [here](#).

Index Terms: bandwidth extension, audio super-resolution, speech synthesis

1. INTRODUCTION

Audio super-resolution, also referred to as Bandwidth Extension (BWE), is the task of generating an audio waveform at a higher sampling rate from its corresponding low-resolution signal [1]. High resolution audio contains greater detail, resulting in a crispier and a more natural sound overall.

Due to hardware or transmission limitations, it is common that a speech signal’s frequency bandwidth is reduced when transmitted via telecommunication systems. Furthermore, most deep learning based methods for generating audio, both in speech and music domains, are limited to a target audio of low resolution. For instance, in [2] audio is generated from descriptive text captions at a target rate of 16 kHz. This results in losing most of the signal’s richness and fidelity, yielding poor user experience. As many audio applications and post-processing tools today benefit from using the full frequency bandwidth, BWE is an important task in itself for audio and video calls, and can also be beneficial for generative audio systems and post-processing pipelines.

Over the last decades, a plethora of research showed success in BWE. Early works base their solutions on the source-

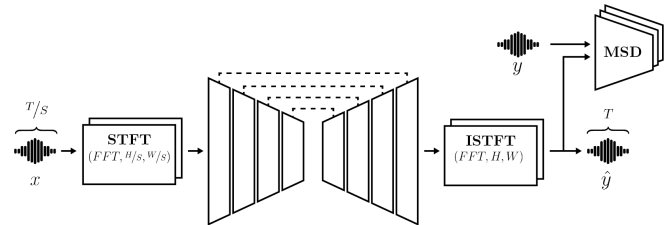


Fig. 1: A waveform of length T/s is converted to the complex-as-channels spectrogram via STFT with scaled down hop and window sizes: $H/s, W/s$. After passing through a U-Net-like model, the signal is converted back to a waveform of length T via iSTFT with hop and window sizes: H, W . During training, a set of multi-scale discriminators (MSD) are utilized for adversarial and feature losses in the time domain, together with a spectral reconstruction loss.

filter model [1]. Generative methods that utilize neural networks provide statistical and data-driven solutions that excel in generating high-frequency signals. Early methods are trained by minimizing a reconstruction loss [3, 4]. Later, generative adversarial networks, diffusion based methods and other generative models showed further success [5, 6, 7, 8, 9].

Neural network based methods either operate on the raw waveform [5, 4, 6, 7, 8] or on some spectral representation of the signal: Line Spectral Frequencies (LSF) [10], magnitude spectrogram [11] or the log-power magnitude spectrogram [3, 12]. The length of audio signals, especially at high resolution, is extremely long, hence modeling it is computationally expensive; this is especially relevant in time-domain based methods. Spectral-based methods face the following challenges: (i) utilizing the phase information from the input, and (ii) reusing the low-frequency bands of the input signal in the reconstructed signal. The authors in [3, 12] resolve (i) by flipping the existing low-resolution phase, whereas [13] applies a designated neural network to directly estimate the high-frequency phase. Typical spectral-based approaches [3, 12, 11, 13] resolve (ii) by generating only the high-frequency spectral features and reusing the low-frequency features via concatenation. This may cause artifacts at the verge between existing and generated frequency bands.

In this work we propose a method for generating high-frequency content in the spectral domain. Inspired by recent success of the Demucs architecture on music source separation and speech enhancement [14, 15, 16], the proposed

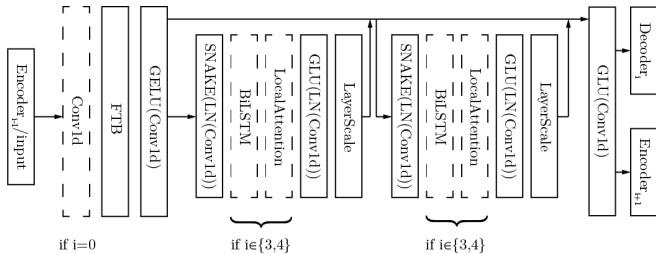


Fig. 2: Encoder layer.

method is composed of a convolutional U-Net model that operates solely in the frequency domain, together with a set of reconstruction, adversarial and feature losses that operate on the spectral and time representations of the signal. Similar to [17], the model operates on the Complex-as-Channel representation of the complex-valued spectrogram [18], thus jointly utilizing both magnitude and phase information and avoiding the need to separately reconstruct the phase of the high-frequency signal. Furthermore, we introduce a way to upsample a signal in the spectral domain that avoids concatenation between existing and generated frequency bands. The proposed method is illustrated in Figure 1.

We empirically show that the proposed method surpasses current state-of-the-art methods. We perform ablation studies to investigate how objective and subjective metrics are impacted by different components of the U-Net model and by the various losses used.

2. METHOD

Given a signal of low resolution $x \in \mathbb{R}^{T/s}$ that was downsampled from its high-resolution counterpart $y \in \mathbb{R}^T$, where s is a fixed upsampling scaling factor, our goal is to reconstruct $\hat{y} \approx y$ and generate its missing high-frequency content.

Operating in the frequency domain, the waveform signal x is converted to X using short-time Fourier transform (STFT). As demonstrated in [18], the input to the model is represented as a concatenation of the real and imaginary parts of the complex-valued spectrogram. The model is then trained to directly predict the spectrogram of the high-frequency signal. The resulting spectrogram \hat{Y} is then transformed back to the reconstructed high-resolution signal \hat{y} using the inverse short-time Fourier transform (iSTFT).

2.1. Architecture

Inspired by Demucs [14], our model is a convolutional U-Net architecture that operates in the frequency domain, with four layers in the encoder and decoder each. The encoder accepts the signal in spectrogram form, and uses 1D convolutions that operate only on the frequency axis. A Frequency Transformer Block (FTB) [19] is added before each encoder layer. Within each layer are two compressed residual branches; as opposed

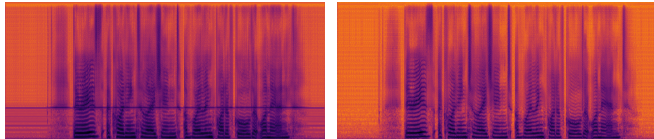


Fig. 3: Spectral upsampling comparison. Both spectrograms are outputs of the same signal resulting from the model before the iSTFT stage, upsampled from 4kHz to 16kHz. The left spectrogram is generated with no spectral upsampling, whereas the one on the right is generated with spectral upsampling.

to the original Demucs architecture, we use the Snake activation function [20]. For the inner layers of the encoder we utilize both LSTM and temporal-based attention modules. With a downsampling scheme of [4,4,2,2], the resulting latent vector is a projection of the input spectrogram, compressed 64-fold in the frequency axis. The encoder layer is visually described in Figure 2. Following the encoder, a decoder transforms the latent vector to a spectrogram of size equal to that of the input to the encoder.

Unlike prior studies that first perform upsampling and then optimize the network to fill the missing frequency range [5, 11], in this work we directly multiply the hop-length and the window size of the iSTFT by the scaling factor s (more details can be found in Section 2.3). With the proposed upsampling technique, information in the encoding process is held across the whole range of frequencies instead of being limited by the Nyquist rate. To accommodate for this, we use concatenated skip connections instead of summation.

2.2. Training Objective

Similar to [15], we use a multi-resolution STFT loss [21] using FFT bins $\in \{512, 1024, 2048\}$, hop lengths $\in \{50, 120, 240\}$ and window sizes $\in \{240, 600, 1200\}$. Additionally we apply the multi-scale adversarial and feature losses [5] that operate in the time domain.

Using only a spectral reconstruction loss we substantially outperform state-of-the-art methods in objective metrics. We found that this produces audible artifacts and significantly impacts subjective metrics. Adding adversarial and feature losses acts as a type of perceptual loss and removes artifacts while slightly reducing the objective metrics (see Table 3).

2.3. Upsampling in the Frequency Domain

As mentioned above, a typical first step in audio upsampling methods is to upsample the input signal to the target sample rate in the time domain using Sinc interpolation [22, 11, 8, 5, 7, 6]. The resulting waveform potentially holds the Nyquist rate of a high-resolution signal, but, as no additional frequencies are actually added, the top segment of the corresponding spectrogram holds no significant information. We find that this technique produces significant artifacts at the verge between the observed low-frequency range and the generated high-frequency range, as seen in Figure 3.

Table 1: L, V and M denote LSD, ViSQOL and MUSHRA respectively. MUSHRA score is specified with a \pm Confidence Interval of 0.95.

	8-16			8-24			4-16			11-44		
	L↓	V↑	M↑									
Reference	-	-	96.25±1.5	-	-	97.16±1.4	-	-	96.18±1.5	-	-	95.30±2.5
Anchor	-	-	54.65±4.3	-	-	56.21±4.4	-	-	41.14±3.8	-	-	46.55±7.4
Sinc	2.32	3.41	60.13±4.7	2.96	3.41	59.49±4.8	3.59	2.27	43.03±3.9	3.91	1.97	47.61±8.0
TFiLM [4]	1.27	3.18	58.53±4.0	-	-	-	1.77	2.25	41.91±4.0	-	-	-
SEANet [5]	0.79	4.08	91.23±2.9	0.91	4.06	94.16±2.2	0.99	3.16	89.40±3.2	1.13	2.88	80.52±7.0
BEHMGAN [17]	-	-	-	-	-	-	-	-	-	1.80	2.01	46.27±8.3
Ours (²⁵⁶ / ₅₁₂)	0.84	4.02	90.58±2.3	0.99	4.03	96.40±1.9	1.04	3.04	86.14±3.4	1.16	2.88	81.21±6.4
Ours (¹²⁸ / ₅₁₂)	0.80	4.11	92.63±2.4	0.91	4.12	95.41±2.0	0.99	3.15	92.05±2.7	1.16	2.89	81.67±6.8
Ours (⁶⁴ / ₅₁₂)	0.77	4.16	94.64±1.6	0.90	4.17	94.45±2.1	0.94	3.28	90.61±3.1	1.12	2.88	84.18±5.6

Table 2: 12-48 results. We use the ²⁵⁶/₁₀₂₄ configuration.

	L↓	V↑	M↑
Reference	-	-	98.47±0.9
Anchor	-	-	67.76±4.1
Sinc	3.36	4.33	69.77±4.3
SEANet [5]	0.86	4.71	96.17±1.6
NuWave2 [8]	1.34	4.42	84.87±4.5
Ours	0.92	4.67	96.71±1.8

To mitigate this, we propose a method for upsampling in the frequency domain. Using different window sizes and hop lengths at the STFT and iSTFT stages, we can start from a given low-resolution signal $x \in \mathbb{R}^{T/s}$ and end with a high-resolution $y \in \mathbb{R}^T$ – upsampled by a factor of s – while using a single STFT representation of fixed size at the intermediate generation stage. With this technique, the input to the model holds information across the whole range of frequencies.

At the STFT stage, the waveform signal x is converted to X with f frequency bins, a hop length of $\frac{f/k}{s}$, and a window length of $\frac{f}{s}$, where k defines the overlapping ratio between consecutive frames. At the iSTFT stage, the model’s output \hat{Y} is transformed to \hat{y} using parameters customized to the upsampling setting; this uses the same number of frequency bins f , but with a hop length of f/k and a window length of f . This process is illustrated in Figure 1.

3. EXPERIMENTS

We test the performance of our model on speech signals from VCTK [23] under different upsampling settings: 4-16 kHz, 8-16 kHz, 8-24 kHz, and 12-48 kHz. In addition to speech signals, we test our model on music signals from MusDB [24] in a setting of 11.025-44.1 kHz. We measure our model’s performance using both objective and qualitative measures.

The VCTK dataset [23] contains around 44 hours of speech from 110 speakers, sampled at 48 kHz. The training

and test setup is the same as in [8]: we omit speakers $p280$ and $p315$. Using only recordings from *mic1*, we use the first 100 speakers for training and the remaining 8 speakers for testing.

The MusDB dataset [24] contains 150 songs (10 hours) of musical mixtures, along with isolated stems, sampled at 44.1 kHz. We use the provided train/test setup, using only the mixture tracks to test our model and baselines.

3.1. Baselines

We compare the proposed method to several audio super resolution methods. For speech data, we compare against SEANet [5], TFiLM [4], and NuWave2 [8]. For musical data we compare against SEANet and BEHM-GAN [17]. We additionally include a comparison to a naive Sinc interpolation method using the `torchaudio` package.

3.2. Model Evaluation

Two objective metrics and a qualitative metric are used to measure the quality of the reconstructed audio with respect to the reference signal:

Log Spectral Distance (LSD) denoting the log-spectral power magnitudes \hat{Y} and Y of signals \hat{y} and y , defined as $Y(\tau, \kappa) = \log_{10} |S(y)|^2$ where S is the STFT, with the Hanning window of 2048 samples and hop length of 512. The LSD is defined as:

$$LSD(\hat{y}, y) = \frac{1}{T} \sum_{\tau=1}^T \sqrt{\frac{1}{K} \sum_{\kappa=1}^K (\hat{Y}(\tau, \kappa) - Y(\tau, \kappa))^2}.$$

Virtual Speech Quality Objective Listener (ViSQOL) is a signal-based, full-reference, intrusive metric that models human speech quality perception using a spectro-temporal measure of similarity between a reference and a test speech signal (from 1 to 5) [25]. The MusDB setting was evaluated using the audio mode configuration.

MULTI Stimulus test with Hidden Reference and Anchor (MUSHRA) is a qualitative subjective assessment of intermediate quality level of audio systems. We used a web platform

Table 3: Adversarial ablation study

Setting	LSD ↓	VISQOL ↑	MUSHRA ↑
Reference	-	-	92.49±2.2
Anchor	-	-	32.34±3.3
No disc.	0.8793	3.363	32.46±3.5
1 MSD	0.978	3.202	85.79±3.0
3 MSD	0.943	3.275	85.57±2.9
Only feat. loss	0.986	3.253	77.64±3.7
Only adv. loss	1.012	3.018	73.96±4.0

[26] to perform a human listening test, asking users to rate the quality of recordings in the range of 0 to 100 [27].

3.3. Results

In all experiments, we trained our model for 500K steps. For the baseline methods, we followed the recommended hyper-parameters recipes provided by the authors.

In settings with a target sampling frequency of up to 44.1 kHz, we use a batch-size of 16, $\frac{\text{hop length}}{\text{window size}}$ ratios of $k \in \{\frac{1}{2}, \frac{1}{4}, \frac{1}{8}\}$ and 512 frequency bins. For the 12-48 kHz setting, we use a batch-size of 8, $k = \frac{1}{4}$, and 1024 frequency bins.

Results are summarized in Tables 1 and 2. The results suggest that the proposed method is superior to the evaluated baselines considering both objective and subjective metrics. Note that under the 4-16 kHz setting, we outperform all methods by a significant margin with $\frac{\text{hop length}}{\text{window size}}$ ratio of $k = \frac{1}{8}$, with $k = \frac{1}{4}$ we are comparable with the adversarial method SEANet in objective metrics, while surpassing it subjectively, whereas with $k = \frac{1}{2}$ we are surpassed by it.

3.4. Ablation Study

We study the effect of the different discriminators and encoder components on the overall model performance.

Impact of Discriminators. We investigate the usage of different number of Multi-Scale Discriminators (MSD), adversarial and feature losses, both jointly and each separately, and how they impact objective and subjective metrics. Results are reported in Table 3. We note that while the non-adversarial setting provides the best objective results, it significantly under-performs in the subjective tests. The model with three MSD with a combination of both adversarial and feature losses ranked second in objective metrics, but is slightly surpassed by the similar single discriminator setting in the subjective tests. We conclude that both feature and adversarial losses are crucial to the success of the task, whereas the exact number of MSD used is less crucial.

Component Analysis. We investigate the choice of activation function, upsampling technique, the usage of the FTB module and their impact on the objective metrics. Results are reported in Table 4. While the study shows no significant improvement provided by individual components, the overall contribution

Table 4: Component ablation study. We report LSD and ViSQOL results for different model configuration. Under the Upsampling column "spec." denotes the proposed method and "time" denotes a pre-upsampling stage via Sinc interpolation.

	Activation	Upsampling	FTB	LSD ↓	VISQOL ↑
1	ReLU	spec.	yes	0.945	3.262
2	ReLU	spec.	no	0.952	3.273
3	ReLU	time	yes	0.957	3.263
4	ReLU	time	no	0.948	3.249
5	Snake	spec.	yes	0.943	3.275
6	Snake	spec.	no	0.958	3.243
7	Snake	time	yes	0.947	3.267
8	Snake	time	no	0.977	3.245

of all the components provides the optimal results. As seen in Figure 3, using spectral upsampling produces a finer transition from the observed and generated frequency ranges.

Impact of Hop Length Size. The choice of $\frac{\text{hop length}}{\text{window size}}$ for $k \in \{\frac{1}{2}, \frac{1}{4}, \frac{1}{8}\}$ defines the length of the signal in the spectral domain, which impacts the computational cost during training and inference. We tested training times on the VCTK’s 8-16 kHz setting, and inference time on 5 songs from the musical 11-44 kHz setting, on a single Nvidia A5000 GPU. Comparing to $k = \frac{1}{8}$, we record an improvement by a factor of 1.4 and 2.03 in average training time per epoch, and 3.35 and 8.43 in average inference time, for $k = \frac{1}{4}, \frac{1}{2}$ respectively. As observed in Table 1, we see a decline in objective metrics as k increases. For every k , under all settings, our method is subjectively comparable or improves, with respect to the best evaluated baseline – SEANet.

4. CONCLUSIONS & FUTURE WORK

In this work we proposed an encoder-decoder method operating over the complex-valued spectrogram for audio super-resolution. We evaluate the proposed method using different upsampling factors considering both speech and music data. We empirically show that the proposed method is superior to the evaluated baselines considering objective and subjective metrics, and we conclude with an ablation study to better assess the contribution of each of the models’ components to the model performance.

For future work, we would like to explore the possibility to convert the proposed method to real-time and streaming processing. Additionally, we would like to train such models considering multi-task setups, e.g., jointly upsampling and denoising the input signal.

Acknowledgements

This research is supported by the *science accelerator* program by the Ministry of Science and Technology, Israel.

5. REFERENCES

- [1] Bernd Iser et al., *Bandwidth extension of speech signals*, Springer, 2008.
- [2] Felix Kreuk et al., “Audiogen: Textually guided audio generation,” 2022.
- [3] Kehuang Li and Chin-Hui Lee, “A deep neural network approach to speech bandwidth expansion,” in *2015 IEEE International Conference on Acoustics, Speech and Signal Processing (ICASSP)*, 2015, pp. 4395–4399.
- [4] Volodymyr Kuleshov et al., “Audio super-resolution using neural networks,” in *ICLR (Workshop)*, 2017.
- [5] Yunpeng Li et al., “Real-time speech frequency bandwidth extension,” in *ICASSP 2021 - 2021 IEEE International Conference on Acoustics, Speech and Signal Processing (ICASSP)*, 2021.
- [6] Sung Kim and Visvesh Sathe, “Bandwidth extension on raw audio via generative adversarial networks,” 2019.
- [7] Jiaqi Su et al., “Bandwidth extension is all you need,” in *ICASSP 2021 - 2021 IEEE International Conference on Acoustics, Speech and Signal Processing (ICASSP)*, 2021, pp. 696–700.
- [8] Seungu Han and Junhyeok Lee, “NU-Wave 2: A General Neural Audio Upsampling Model for Various Sampling Rates,” in *Proc. Interspeech 2022*, 2022, pp. 4401–4405.
- [9] Kexun Zhang, Yi Ren, Changliang Xu, and Zhou Zhao, “WSRGlOW: A Glow-Based Waveform Generative Model for Audio Super-Resolution,” in *Proc. Interspeech 2021*, 2021, pp. 1649–1653.
- [10] Sen Li et al., “Speech bandwidth extension using generative adversarial networks,” in *2018 IEEE International Conference on Acoustics, Speech and Signal Processing (ICASSP)*, 2018.
- [11] Rithesh Kumar et al., “Nu-gan: High resolution neural upsampling with gan,” 2020.
- [12] Sefik Emre Eskimez and Kazuhito Koishida, “Speech super resolution generative adversarial network,” in *IEEE International Conference on Acoustics, Speech and Signal Processing (ICASSP)*, 2019.
- [13] Shichao Hu et al., “Phase-Aware Music Super-Resolution Using Generative Adversarial Networks,” in *Proc. Interspeech 2020*, 2020, pp. 4074–4078.
- [14] Alexandre Défossez, “Hybrid spectrogram and waveform source separation,” in *Proceedings of the ISMIR 2021 Workshop on Music Source Separation*, 2021.
- [15] Alexandre Défossez et al., “Real time speech enhancement in the waveform domain,” in *Interspeech 2020*, 2020, ISCA.
- [16] Arnon Turetzy et al., “Deep audio waveform prior,” in *Interspeech 2022*, 2022, ISCA.
- [17] Eloi Moliner and Vesa Välimäki, “Behm-gan: Bandwidth extension of historical music using generative adversarial networks,” 2022.
- [18] Woosung Choi et al., “Investigating u-nets with various intermediate blocks for spectrogram-based singing voice separation,” in *21th International Society for Music Information Retrieval Conference, ISMIR*, Ed., 2020.
- [19] Dacheng Yin et al., “Phasen: A phase-and-harmonics-aware speech enhancement network,” *Proceedings of the AAAI Conference on Artificial Intelligence*, vol. 34, no. 05, pp. 9458–9465, Apr. 2020.
- [20] Liu Ziyin et al., “Neural networks fail to learn periodic functions and how to fix it,” in *Advances in Neural Information Processing Systems*, H. Larochelle, M. Ranzato, R. Hadsell, M.F. Balcan, and H. Lin, Eds. 2020, vol. 33, pp. 1583–1594, Curran Associates, Inc.
- [21] Ryuichi Yamamoto et al., “Parallel wavegan: A fast waveform generation model based on generative adversarial networks with multi-resolution spectrogram,” in *ICASSP 2020 - 2020 IEEE International Conference on Acoustics, Speech and Signal Processing (ICASSP)*, 2020, pp. 6199–6203.
- [22] Sawyer Birnbaum et al., “Temporal film: Capturing long-range sequence dependencies with feature-wise modulations,” in *Advances in Neural Information Processing Systems*, 2019, Curran Associates, Inc.
- [23] Junichi Yamagishi et al., “Cstr vctk corpus: English multi-speaker corpus for cstr voice cloning toolkit,” 2019.
- [24] Zafar Rafii et al., “Musdb18-hq - an uncompressed version of musdb18,” 2019.
- [25] Andrew Hines et al., “Visqol: an objective speech quality model,” *EURASIP Journal on Audio, Speech, and Music Processing*, vol. 2015, no. 1, pp. 1–18, 2015.
- [26] Michael Schoeffler et al., “webmushra — a comprehensive framework for web-based listening tests,” *Journal of Open Research Software*, vol. 6, no. 1, pp. 8, 2018.
- [27] ITU, “Itu-r rec. bs.1534-3: Subjective assessment of sound quality,” 2015.